



HAL
open science

Trefftz approximation space for Poisson equation in perforated domains

Miranda Boutilier, Konstantin Brenner, Victorita Dolean

► **To cite this version:**

Miranda Boutilier, Konstantin Brenner, Victorita Dolean. Trefftz approximation space for Poisson equation in perforated domains. 2023. hal-04072474

HAL Id: hal-04072474

<https://hal.science/hal-04072474>

Preprint submitted on 18 Apr 2023

HAL is a multi-disciplinary open access archive for the deposit and dissemination of scientific research documents, whether they are published or not. The documents may come from teaching and research institutions in France or abroad, or from public or private research centers.

L'archive ouverte pluridisciplinaire **HAL**, est destinée au dépôt et à la diffusion de documents scientifiques de niveau recherche, publiés ou non, émanant des établissements d'enseignement et de recherche français ou étrangers, des laboratoires publics ou privés.

Trefftz approximation space for Poisson equation in perforated domains

Miranda Boutilier¹, Konstantin Brenner², and Victorita Dolean³

¹ Université Côte d'Azur, LJAD

² Université Côte d'Azur, LJAD, CNRS, INRIA

³ University of Strathclyde, Dept. of Maths and Stats and Université Côte d'Azur, LJAD, CNRS

Abstract. For the Poisson equation posed in a planar domain containing a large number of polygonal perforations, we propose a low dimensional approximation space based on a coarse polygonal partitioning of the domain. Similar to other multi-scale numerical methods, this coarse space is spanned by basis functions that are locally discrete harmonic. We provide an error estimate in the energy norm that only depends on the regularity of the solution over the edges of the coarse skeleton. For a specific edge refinement procedure, this estimate allows to establish the superconvergence of the method even if the true solution has a low general regularity. Combined with the Restricted Additive Schwarz method, the proposed coarse space leads to an efficient two-level iterative linear solver which achieves the fine-scale finite element error in few iterations. The numerical experiment showcases the use of this coarse space over the test cases involving singular solutions and realistic urban geometries.

Keywords: Multi-scale finite element method, Trefftz method, Domain Decomposition

1 Introduction

Let D be an open simply connected polygonal domain in \mathbb{R}^2 , we denote by $(\Omega_{S,k})_k$ a finite family of perforations in D such that each $\Omega_{S,k}$ is an open connected polygonal subdomain of D . The perforations are mutually disjoint such that $\overline{\Omega_{S,k}} \cap \overline{\Omega_{S,l}} = \emptyset$ for any $k \neq l$. We denote $\Omega_S = \bigcup_k \Omega_{S,k}$ and $\Omega = D \setminus \overline{\Omega_S}$, assuming that the family $(\Omega_{S,k})_k$ is such that Ω is connected. Note that the latter assumption implies that $\Omega_{S,k}$ are simply connected.

In this contribution we consider the following model problem

$$\begin{cases} -\Delta u = f & \text{in } \Omega, \\ \frac{\partial u}{\partial \mathbf{n}} = 0 & \text{on } \partial\Omega \cap \partial\Omega_S, \\ u = 0 & \text{on } \partial\Omega \setminus \partial\Omega_S. \end{cases} \quad (1)$$

Our motivation behind this linear problem lies in the applications to urban flood modeling. In this context u would represent the flow potential (pressure

head) and $(\Omega_{S,k})_k$ can be thought of as a family of impervious structures such as buildings, walls, etc. Although the problem (1) is overly simplified to be directly used for urban hydraulic modeling, the more general nonlinear elliptic or parabolic models are common in free surface flow simulations. Such models arise from Shallow Water equations either by neglecting the inertia terms [1] or within the context of semi-implicit Froude-robust time discretizations [6].

One of the challenges of the numerical modeling of urban floods is that the small structural features may significantly affect the flow. Luckily, modern terrain survey techniques allow to acquire high-resolution topographic data, for example, the data set used in this article provided by Métropole Nice Côte d’Azur allows for the infra-metric description of the urban geometries [2].

Depending on the geometrical complexity of the computational domain, the numerical resolution of (1) may become increasingly challenging. In this regard, we propose two main approaches to efficiently solve the model problem. Both methods consider two “levels” of space discretization (see Figure 1). The first level will be based on a coarse polygonal partitioning of Ω , while the second one is associated with the fine-scale triangulation and is designed to resolve the small scale details of the model domain. The coarse polygonal partitioning is first used to decompose the solution of (1) into the sum of a locally harmonic function combined with local subdomain contributions that can be efficiently computed in parallel. This splitting leads to a system that can be seen as a continuous version of the Schur complement problem. We then introduce a low-dimensional space that serves to approximate the locally harmonic component of the solution. This coarse approximation space, called here Trefftz or discrete Trefftz space, is built upon basis functions that satisfy the local Laplace problems either exactly or via a finite element approximation. Here, the basis functions have piecewise linear traces along the edges of the coarse mesh. We note that this coarse space can be readily extended to use higher-order polynomials on the coarse edges.

The first approach that we are going to investigate involves approximating the locally harmonic component of the solution (or the solution itself) within the coarse space. In a way our methodology is similar to MsFEM [8], VEM [5] or methods combining boundary elements and finite elements (BEM-FEM) [9]. Compared to VEM, the major difference is that we do compute the approximation of the locally harmonic basis. By doing so, we manage to incorporate into the coarse space the singular functions corresponding to the corners of the domain. We are also able to deal with very general polygonal cells (not star-shaped, not simply connected, etc.), which differs our approach from both VEM and BEM-FEM. Additionally, we willingly avoid using a method of fundamental solutions of any kind, because of our long-term motivation in problems more complex than (1). In comparison to the classical MsFEM, the resonance error is avoided thanks to a priori geometrical fitting of the coarse degrees of freedom. Finally, our coarse approximation strategy can be interpreted as a primal version of the MHM method [3].

The second approach combines the coarse approximation with local subdomain solves in a two-level Domain Decomposition method. This results in an

efficient iterative solver for the algebraic system resulting from the fine-scale finite element method. The obtained algorithm can also be thought as a way of improving the precision of the original coarse approximation in the spirit of iterative multi-scale methods (see e.g. [7]). We note that alternatively, the discrete Trefftz coarse space can be used as a component of a two-level preconditioner for a Krylov method. This approach has been investigated in our previous article [4].

2 Schur complement problem and Trefftz approximation

We begin with a coarse discretization of Ω which involves a family of polygonal cells $(\Omega_j)_{j=1,\dots,N}$, the so-called coarse skeleton Γ , and the set of coarse grid nodes that will be referred to by \mathcal{V} . The construction is as follows. Consider a finite nonoverlapping polygonal partitioning of D denoted by $(D_j)_{j=1,\dots,N}$ and an induced nonoverlapping partitioning of Ω denoted by $(\Omega_j)_{j=1,\dots,N}$ such that $\Omega_j = D_j \cap \Omega$. We will refer to $(\Omega_j)_{j=1,\dots,N}$ as the coarse mesh over Ω . Additionally, we denote by Γ its skeleton, that is $\Gamma = \bigcup_{j=1,\dots,N} \partial\Omega_j \setminus \partial\Omega_S$.

Based on the coarse partitioning and with the problem (1) in mind, we split $H^1(\Omega)$ into a direct sum of its subspaces $H_\Delta^1(\Omega)$ and $H_\Gamma^1(\Omega)$. Here, $H_\Gamma^1(\Omega)$ is a subspace of functions vanishing at Γ and $H_\Delta^1(\Omega)$ its H^1 -orthogonal complement made of locally harmonic functions. Using the orthogonal decomposition introduced above we can express the weak formulation of (1) as the following Schur complement problem: Find $u = u_\Delta + u_b$ with $u_\Delta \in \cap H_{\partial\Omega \setminus \partial\Omega_S}^1(\Omega)$ and $u_b \in H_\Gamma^1(\Omega)$ satisfying

$$\begin{cases} (u_\Delta, v)_{H^1(\Omega)} = (f, v)_{L^2(\Omega)} & \forall v \in H_\Delta^1(\Omega) \cap H_{\partial\Omega \setminus \partial\Omega_S}^1(\Omega), \\ (u_b, v)_{H^1(\Omega)} = (f, v)_{L^2(\Omega)} & \forall v \in H_\Gamma^1(\Omega). \end{cases} \quad (2)$$

We remark that the local ‘‘bubble’’ component of the solution u_b can be computed from (2) locally (and in parallel) on each Ω_j , while the problem for u_Δ is globally coupled over Ω .

We now proceed with the approximation of the locally harmonic component u_Δ . For this, we introduce the Trefftz coarse space, a finite-dimensional subspace V_H of $H_\Delta^1(\Omega)$ that is spanned by the functions that are piecewise linear on the skeleton Γ . Let $(e_k)_{k=1,\dots,N_e}$ denote a nonoverlapping partitioning of Γ such that each ‘‘coarse edge’’ e_k is an open planar segment, and we denote $H = \max_{k=1,\dots,N_e} |e_k|$. We note that a straight segment of Γ may be subdivided into multiple edges (see Figure 4). The set of coarse grid nodes is given by $\mathcal{V} = \bigcup_{k=1,\dots,N_e} \partial e_k$.

The coarse nodal basis is defined by the following set of boundary value problems. For all Ω_j and for all $s = 1, \dots, N_\mathcal{V}$, find $\phi_s^j \in H^1(\Omega_j)$ such that ϕ_s^j is the weak solution to the following problem

$$\begin{cases} \Delta \phi_s^j = 0 & \text{in } \Omega_j, \\ \frac{\partial \phi_s^j}{\partial \mathbf{n}} = 0 & \text{on } \partial\Omega_j \cap \partial\Omega_S, \\ \phi_s^j = g_s & \text{on } \partial\Omega_j \setminus \partial\Omega_S, \end{cases} \quad (3)$$

where g_s is a skeleton “hat” basis function, that is $g_s : \Gamma \rightarrow \mathbb{R}$ is continuous on Γ , linear on each edge e_k and satisfies $g(\mathbf{x}_i) = \delta_{is}$ for all nodes \mathbf{x}_i .

Let $V_{H,0} = V_H \cap H^1_{\partial\Omega \setminus \partial\Omega_S}(\Omega)$. The Galerkin method based on the coarse space reads as follows: find $u_H \in V_{H,0}$ such that

$$(u_H, v_H)_{H^1(\Omega)} = (f, v_H)_{L^2(\Omega)} \quad \forall v_H \in V_{H,0}. \quad (4)$$

Combining best approximation property of the coarse approximation u_H , classical finite element interpolation theory in one dimension, and an interpolation inequality we obtain the following error estimate for the approximation of u_Δ .

Proposition 21 *Assume that there exists a finite nonoverlapping partitioning $(\gamma_l)_{l=1,\dots,N_\gamma}$ of Γ such that the traces of u belong to $H^2(\gamma_l)$ for all l ; assume in addition that the set of coarse edges $(e_k)_k$ is a subdivision of $(\gamma_l)_l$. There exists $C > 0$ depending only on $(\Omega_j)_j$ and $(\gamma_l)_l$ such that*

$$\|\nabla(u_\Delta - u_H)\|_{L^2(\Omega)} \leq CH^{\frac{3}{2}} \left(\sum_{l=1}^{N_\gamma} \|u\|_{H^2(\gamma_l)}^2 \right)^{\frac{1}{2}}. \quad (5)$$

We remark that the broken H^2 norm in the right-hand side of (5) involves only the traces of the solution along the sections of the coarse skeleton. Therefore, this estimate is valid for u having low general regularity that is due, for example, to corner singularities. As a matter of fact, the estimate (5) provides an a priori criterion for the adaptation of the coarse mesh: one has to ensure that the edge norm in the right-hand side is small. For f regular enough, this can be achieved by moving the coarse edges away from the “bad” perforation corners. We further note that this estimate is especially valuable for a so-called space or edge refinement, which is a procedure that involves splitting the edges of an otherwise fixed coarse grid. In that case, one observes the superconvergence of the error with a rate of $3/2$.

3 Discrete Trefftz space and two-level Schwarz method

Let us consider the triangulation of Ω which is assumed to be conforming with respect to the polygonal partitioning $(\Omega_j)_{j=1,\dots,N}$ (see Figure 1). We denote by V_h the space of piecewise linear continuous function over this triangulation, where h denotes the maximal element diameter. The associated “fine-scale” finite element discretization of (1) results in the linear system $\mathbf{A}\mathbf{u} = \mathbf{f}$. Because the triangular mesh resolves the fine-scale structure (the perforations), the latter system may be quite large; moreover the size of the triangular elements may vary by several orders of magnitude. As a result the matrix \mathbf{A} is expected to be poorly conditioned. Below, we will show how the coarse space introduced in the previous section can be combined with RAS to construct a simple yet efficient iterative linear solver for the fine-scale finite element method.

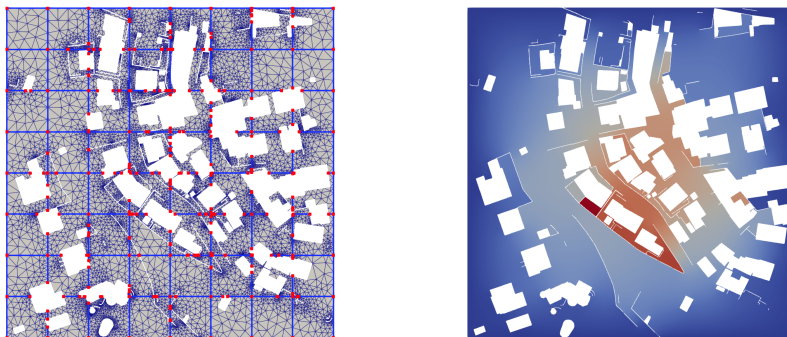


Fig. 1: Left: coarse (thick lines) and fine (thin lines) discretizations, with the coarse nodes shown by red dots. Right: finite element solution with $f = 1$.

Let us begin with the coarse space component. In most practical situations, the coarse basis functions defined by (3) cannot be computed analytically. Therefore, we consider the finite element approximation of V_H denoted by $V_{H,h}$. The basis of the discrete Trefftz space is obtained through the finite element approximation of (3). Let \mathbf{R}_H be a transition matrix from the discrete Trefftz basis of $V_{H,h}$ toward the standard finite element nodal basis of V_h . The finite element counterpart of (4) can be expressed algebraically as $\mathbf{u}_H = M_H^{-1}\mathbf{f}$, where $M_H^{-1} = \mathbf{R}_H^T (\mathbf{R}_H \mathbf{A} \mathbf{R}_H^T)^{-1} \mathbf{R}_H$.

Let $(\Omega'_j)_{j=1,\dots,N}$ denote the overlapping partitioning of Ω such that $\Omega_j \subset \Omega'_j$. In practice, each Ω'_j is constructed by propagating Ω_j by a few layers of triangles. Consider classical boolean restriction matrices \mathbf{R}'_j associated to the family $(\Omega'_j)_{j=1,\dots,N}$. We introduce the following iterative procedure

$$\begin{aligned} \mathbf{u}^{n+1/2} &= \mathbf{u}^n + M_H^{-1}(\mathbf{f} - \mathbf{A}\mathbf{u}^n) \\ \mathbf{u}^{n+\frac{1}{2}} &= \mathbf{u}^{n+\frac{1}{2}} + M_{RAS}^{-1}(\mathbf{f} - \mathbf{A}\mathbf{u}^{n+\frac{1}{2}}) \end{aligned} \quad (6)$$

where $M_{RAS}^{-1} = \sum_{j=1}^N (\mathbf{R}'_j)^T \mathbf{D}_j (\mathbf{A}'_j)^{-1} \mathbf{R}'_j$ and $\mathbf{A}'_j = \mathbf{R}'_j \mathbf{A} (\mathbf{R}'_j)^T$, while \mathbf{D}_j denote the partition-of-unity matrices.

4 Numerical Results

In this section, we illustrate the performance of the discrete Trefftz space within two different scenarios involving either a standalone Galerkin approximation (4) or an iterative approach (6). In particular, we will provide numerical evidence of the error estimate (5) over the case involving a solution with a corner singularity. The numerical investigation of the iterative algorithm (6) shows that the fine-scale finite element error can be achieved in few iterations.

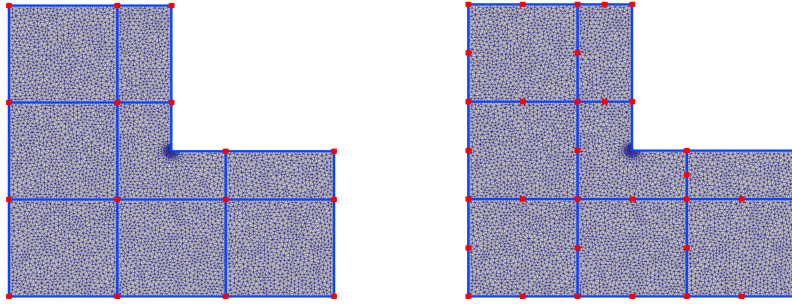


Fig. 2: Coarse and fine discretizations of the L-shaped domain with varying degrees of edge refinement.

Convergence of discrete Trefftz approximation method: We begin with a test case involving a classical L-shaped domain with a reentering corner (Figure 2). The domain is defined by $D = (-1, 1)^2$, $\Omega_S = (0, 1)^2$ and $\Omega = D \setminus \overline{\Omega_S}$. We consider the problem (1) with zero right-hand side and a non-homogeneous Dirichlet boundary condition on $\partial\Omega \setminus \partial\Omega_S$ provided by the singular exact solution $u(r, \theta) = r^{\frac{2}{3}} \cos(\frac{2}{3}(\theta - \pi/2))$.

In order to assess the convergence of the discrete Trefftz method, we consider two strategies regarding the refinement of the coarse partitioning. The procedure involving the reduction of the diameter of the coarse cells will be referred to as *mesh refinement*. The sequence of such meshes will be constructed as follows: first the background domain D is partitioned into $N = (2p + 1)^2$, $p \in \mathbb{N}$, squares, then the coarse cells Ω_j are generated by excluding Ω_S . The choice of N being a square of an odd number ensures the consistency of the mesh sequence in terms of the shape of the elements. Alternatively, we consider the *edge refinement* procedure, which accounts for subdividing the edges of an original “ 3×3 grid”. This edge refinement approach is illustrated by Figure 2. Let us stress that under these refinement procedures, none of the coarse grids will have degree of freedom located at the corner $(0, 0)$. As the result, the corner singularity will be captured by the basis functions associated with the L-shaped domain. We also note that in order to improve the precision of the fine-scale finite element method, the size of the triangles is graded in the vicinity of the corner $(0, 0)$.

Figure 3 reports the error in L^2 and the energy norms as the function of maximal coarse edge length H . The black horizontal line represents the typical fine-scale finite element error. As expected, we observe that the convergence of the discrete Trefftz method deteriorates as the coarse error approaches this value. In accordance with the error estimate (5), for the edge refinement, we observe superconvergence in the energy norm with the rate slightly superior to $3/2$. We note that that the convergence rate in L^2 appears to be superior to $5/2$. In contrast, the convergence resulting from the mesh refinement seems to be controlled by the low global regularity of the solution. We observe the convergence rates typical for finite element methods on quasi-uniform meshes.

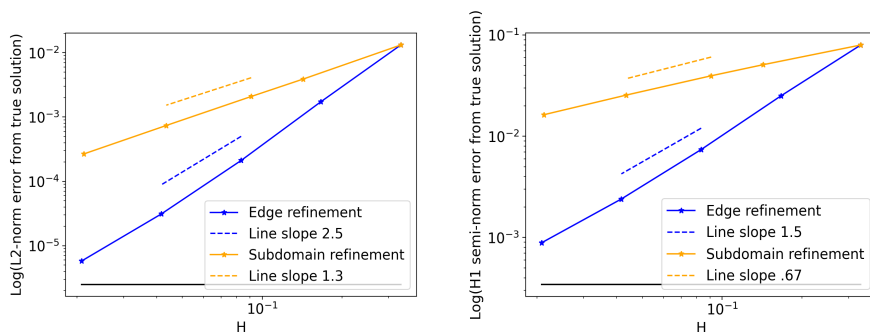


Fig. 3: Coarse approximation error for L-shaped domain with edge (blue) and subdomain (orange) refinement in L^2 norm (left) and the energy norm (right).

Convergence of the two-level iterative method: Next, we examine the performance of the iterative scheme (6) over the L-shaped domain considered previously and a domain based on realistic urban geometries for which the datasets were kindly provided by Métropole Nice Côte d’Azur. The domain involving a small portion of the structural topography of the city of Nice is shown in Figure 1. The dataset contains two kinds of structural elements, namely buildings (and assimilated small elevated structures) and walls.

We report on Figure 4 the convergence history of the iterative method for both L-shaped and urban domains; more precisely, we report the convergence of the full L^2 error, that is the norm of the difference between the intermediate approximation and some accurate solution of (1). Each figure reports the convergence history for linear systems based on increasingly refined background triangulation. The typical width of the overlap in RAS method is of $\text{diam}(\Omega_j)/20$.

For the L-shaped domain, as before, we put $f = 0$ while using the non-homogeneous Dirichlet boundary conditions. For the realistic data set we solve (1) with $f = 1$; the fine-scale finite element solution is reported on Figure 1. As the exact solution is not available for the case based on the urban data, we use a reference numerical solution obtained on a very fine grid.

We observe that the error of the fine-scale finite element method (black lines) can be reached relatively fast. Further iterations do not improve the overall precision of the approximate solution even though the algebraic error may decrease. For the L-shaped domain, the convergence of the full error is essentially exponential; moreover the decay rate of the full error remains consistent with respect to the finite size h of the fine-scale triangulation.

Acknowledgments

This work has been supported by ANR Project Top-up (ANR-20-CE46-0005). The high-resolution structural data has been provided by Métropole Nice Côte

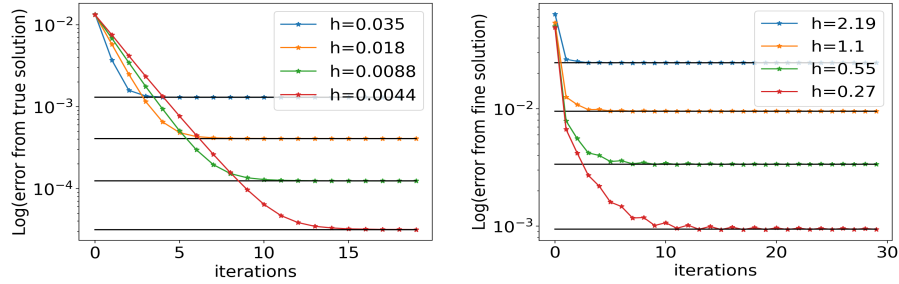


Fig. 4: Convergence of the two-level iterative method for the L-shaped domain on 3×3 subdomains (left) and the urban dataset on 8×8 subdomains (right). The black horizontal lines show the error of the fine-scale finite element method.

d’Azur. We warmly thank Florient Langeron, chief of MNCA’s SIG 3D project, for his help in preparation of the data and for the multiple fruitful discussions.

References

1. Alonso, R., Santillana, M., Dawson, C.: On the diffusive wave approximation of the shallow water equations. *Eur. J. Appl. Math.* **19**(5), 575–606 (2008)
2. Andres, L.: L’apport de la donnée topographique pour la modélisation 3D fine et classifiée d’un territoire. *Rev. XYZ* **133**(4), 24–30 (2012)
3. Araya, R., Harder, C., Paredes, D., Valentin, F.: Multiscale hybrid-mixed method. *SIAM J. Numer. Anal.* **51**(6), 3505–3531 (2013)
4. Boutilier, M., Brenner, K., Dolean, V.: A trefftz-like coarse space for the two-level Schwarz method on perforated domains. *arXiv preprint arXiv:2211.05880* (2022)
5. Brezzi, F., Falk, R.S., Marini, L.D.: Basic principles of mixed virtual element methods. *ESAIM: Mathematical Modelling and Numerical Analysis* **4**(48), 1227–1240 (2014)
6. Casulli, V.: Semi-implicit finite difference methods for the two-dimensional shallow water equations. *Journal of Computational Physics* **86**(1), 56–74 (1990)
7. Hajibeygi, H., Bonfigli, G., Hesse, M.A., Jenny, P.: Iterative multiscale finite-volume method. *Journal of Computational Physics* **19**(277), 8604–8621 (2008)
8. Hou, T.Y., Wu, X.H.: A multiscale finite element method for elliptic problems in composite materials and porous media. *J. Comput. Phys.* **134**(1), 169–189 (1997)
9. Weißer, S.: *BEM-based Finite Element Approaches on Polytopal Meshes*, vol. 130. Springer (2019)